

Ulf Wickström

Introduction

The fire resistance of structural elements is traditionally determined by standard fire endurance tests. However, there is also a need to be able to predict the response of structures of various designs when exposed to alternative design fire conditions. Accurate and robust analytical methods are then needed. Such methods may also be used for predicting standard tests of, for example, structural elements that cannot be tested due to their size or for extending test results to modified structures.

It is necessary when using analytical methods, as well as when interpreting test results and their relations to real fires, to understand the fundamental physics governing the thermal behavior of fire-exposed structures. The focus in this chapter is to meet these needs. The content is based on textbooks on heat transfer theory (e.g., Holman [1] and others) and from various publications in the field of fire safety engineering.

Analytical methods for the design of fire resistance of structures have the following three main components:

1. Determining the duration and level of thermal fire exposure
2. Calculating the heat transfer and the internal temperature distribution
3. Estimating the structural response and the load-bearing capacity

The first step is in general very complex and requires somewhat uncertain assumptions. Most often the fire exposure is assumed according to standardized time-temperature curves, as specified in ISO 834, ASTM E119, or EN 1363-1. Time-temperature developments determined by fire models or measured at ad hoc tests are seldom applied. The next step is very crucial as the deterioration of material strength depends on the temperature obtained. This chapter focuses on this second step. More information on the first and third steps of an analytical design procedure is outlined elsewhere in this section of the handbook.

The temperature calculation methods presented here disregard in general any mechanical failures that may occur that could alter the thermal conditions. Protection systems may, for example, fall off in case of fire exposure and completely change the thermal conditions. Such phenomena must be investigated by full-scale tests and, therefore, new types of structural systems must in general be tested in full scale in standard furnace tests as a basis for type approval and so on. Calculation methods can, however, be used for generalizations or extensions of test results to various dimensions and configurations.

Heat Transfer to Structures

Heat is transferred from hot fire gases to structures by convection and radiation. The

U. Wickström (✉)

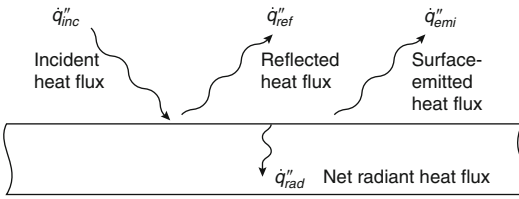


Fig. 34.1 Heat transfer by radiation to a surface, which depends on incident radiation, surface absolute temperature, and surface emissivity

contributions of these two modes of heat transfer are in principal independent and must be treated separately. The convective heat transfer depends on the temperature difference between the target surface and the surrounding gas and the velocity of the gas masses in the vicinity of the exposed surface, whereas the incident heat radiation on a surface originates from surrounding flames and gas masses as well as other surrounding surfaces.

Thus, the total heat flux \dot{q}''_{tot} to a surface is

$$\dot{q}''_{\text{tot}} = \dot{q}''_{\text{rad}} + \dot{q}''_{\text{con}} \quad (34.1)$$

where \dot{q}''_{rad} is the net radiation heat flux and \dot{q}''_{con} is the heat transfer to the surface by convection. Details of these two contributions to follow.

Radiation

The net radiation heat flux \dot{q}''_{rad} depends on the incident radiation \dot{q}''_{inc} , on the surface emissivity/absorptivity, and on the fourth power of the absolute temperature T_s of the targeted surface. The heat exchange at a surface is illustrated in Fig. 34.1.

Part of the incident radiation is absorbed and the rest \dot{q}''_{ref} is reflected. Then the surface emits heat by radiation \dot{q}''_{emi} depending on the emissivity and the surface absolute temperature to the fourth power. Thus, the net radiative heat can be written

$$\dot{q}''_{\text{rad}} = \alpha_s \dot{q}''_{\text{inc}} - \epsilon_s \sigma T_s^4 \quad (34.2)$$

where α_s and ϵ_s are the target surface absorptivity and emissivity, respectively. In this presentation the surface emissivity and absorptivity are assumed equal according to the Kirchoff's identity. Thus,

$$\dot{q}''_{\text{rad}} = \epsilon_s (\dot{q}''_{\text{inc}} - \sigma T_s^4) \quad (34.3)$$

The incident radiation to a surface is emitted by surrounding gas masses and in case of fire by flames and smoke layers and/or by other surfaces. It depends on the fourth power of the absolute temperature. The emissivity and absorptivity of gas masses and flames increase with depth and become, therefore, in general more important in large-scale fires than in, for example, small-scale experiments. In real fires surfaces are exposed to radiation from a large number of sources (surfaces, flames, gas masses, etc.) of different temperatures and emissivities. The heat fluxes are then in general very complicated to model. A simple summation of the main contributions yields in general a good estimate; that is,

$$\dot{q}''_{\text{inc}} = \sum \epsilon_i F_i \sigma T_i^4 \quad (34.4)$$

where ϵ_i is the emissivity of the i th source, F_i and T_i are the corresponding view factor (see Chap. 4, "Radiation Heat Transfer," of this handbook) and temperature, respectively. Equation 34.4 may then be inserted in Equation 34.3 to get

$$\dot{q}''_{\text{rad}} = \epsilon_s \sigma \left(\sum \epsilon_i F_i T_i^4 - T_s^4 \right) \quad (34.5)$$

or

$$\dot{q}''_{\text{rad}} = \epsilon_s \sigma (T_r^4 - T_s^4) \quad (34.6)$$

where T_r is here termed the black body radiation temperature or just the radiation temperature. T_r is a weighted average identified as

$$T_r^4 \equiv \sum \epsilon_i F_i T_i^4 \quad (34.7)$$

The emissivities as used above are surface properties, in principle independent of the fire conditions.

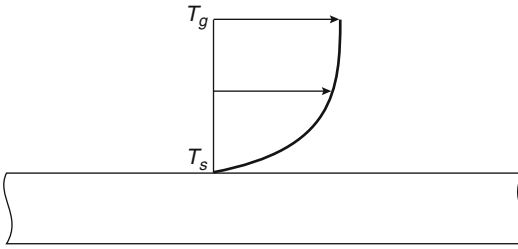


Fig. 34.2 Gas velocity profile, with the heat transfer by convection depending on the temperature difference between the adjacent gases and the target surface and on the gas velocity

Convection

The heat transferred by convection from adjacent gases to a surface varies a lot depending on adjacent gas velocities and geometries (Fig. 34.2).

In most cases it may be written as

$$\dot{q}_{con}'' = h(T_g - T_s)^n \quad (34.8)$$

where h is the convective heat transfer coefficient and T_g is the gas temperature adjacent to the exposed surface. In cases of surfaces heated or cooled by natural or free convection a value of n greater than unity is motivated depending on flow conditions [1].

In fires the heat transfer conditions by convection may vary a lot and the parameters h and n are very hard to determine accurately. However, as radiation heat transfer dominates and the convective conditions are not decisive for the total heat transfer to fire exposed structures, the exponent n is assumed equal to unity for simplicity in most fire engineering cases. Thus,

$$\dot{q}_{con}'' = h(T_g - T_s) \quad (34.9)$$

The convective heat transfer coefficient h depends mainly on flow conditions in the vicinity of the surface and not so much on the surface or the material properties.

Total Heat Transfer and Adiabatic Surface Temperature

The total heat transfer to a surface may now be obtained by adding the contributions by radiation and convection. Thus, by inserting Equations 34.6 and 34.9 into Equation 34.1, the total heat flux to a surface becomes

$$\dot{q}_{tot}'' = \varepsilon_s \sigma (T_r^4 - T_s^4) + h(T_g - T_s) \quad (34.10)$$

In most fire engineering design cases the radiation temperature T_r and the gas temperature T_g are assumed equal to a fire temperature T_f . Then the total heat transfer may be calculated as

$$\dot{q}_{tot}'' = \varepsilon_s \sigma (T_f^4 - T_s^4) + h(T_f - T_s) \quad (34.11)$$

or

$$\dot{q}_{tot}'' = h_{tot}(T_f - T_s) \quad (34.12)$$

where the combined total heat transfer coefficient h_{tot} may be identified from Equations 34.11 and 34.12 as

$$H = \varepsilon_s \sigma (T_f^2 - T_s^2)(T_f + T_s) + h \quad (34.13)$$

Alternatively the two boundary temperatures in Equation 34.10, T_r and T_g , may be combined to one effective temperature T_{AST} , the adiabatic surface temperature. This temperature is defined as the temperature of a surface of an ideally perfectly insulating material, i.e. a surface which cannot absorb any heat [2]. Thus, T_{AST} is defined by the surface heat balance equation

$$\varepsilon_s \sigma (T_r^4 - T_{AST}^4) + h(T_g - T_{AST}) = 0 \quad (34.14)$$

The value of T_{AST} is always between T_r and T_g .

Then the total heat transfer may be written as

$$\dot{q}_{tot}'' = \varepsilon_s \sigma (T_{AST}^4 - T_s^4) + h(T_{AST} - T_s) \quad (34.15)$$

The adiabatic surface temperature T_{AST} can in many cases be measured, and it may be used for calculating heat transfer to fire-exposed surfaces based on practical tests, as discussed later. It can also be obtained from numerical CFD modeling of fires using computer codes like FDS [2, 3].

Heat Transfer to Fire-Exposed Structures

Based on Equations 34.11 and 34.12 the heat transfer to a fire-exposed surface can be calculated for given fire and surface temperatures T_f and T_s . The emissivity ϵ_s is a surface property, which can be assumed to equal 0.8 for most building materials except for shiny steel where a lower value may be assumed. The convection coefficient h is not decisive for the temperature development near a fire-exposed surface of a structure as the radiative heat transfer dominates at high temperatures. In Eurocode 1 [4] a value of $25 \text{ W/m}^2 \text{ K}$ is recommended at fire-exposed surfaces. The temperature on the nonexposed side of a separating structure will, on the other hand, depend very much on the heat transfer conditions including the convection coefficient. In Eurocode 1 in this case a convective heat transfer coefficient value of $4 \text{ W/m}^2 \text{ K}$ is recommended.

In many cases, however, a fire-exposed surface will get temperatures very close to the fire temperature (i.e., $T_f \approx T_s$). This approximation applies for insulation materials with a low density and a low thermal conductivity. It may facilitate calculations considerably and is here applied on calculating temperature in insulated

steel structures (as discussed later). Even a normal weight concrete surface will get a temperature of 90 % of the fire temperature after 30 min (as shown in Fig. 34.19, later in the chapter).

The heat transfer conditions may be very decisive for the temperature development in a fire-exposed bare steel structure (see discussion on unprotected steel structures later in the chapter). They are also very important for the temperature development on the back side of a fire-separating element. This is in particular the case for light weight structures where the thermal insulation properties are decisive rather than the thermal inertia.

Calculating Heat Transfer Using Plate Thermometer Temperatures

So-called *plate thermometers* are used to monitor the temperature in fire resistance furnaces according to the international standard ISO 834 and the European standard EN 1363-1. A plate thermometer (PT) consisting of an Inconel (trade name for a nickel-based superalloy) plate insulated on its back side is shown in Fig. 34.3. A thermocouple fixed to the plate registers its temperature. Figure 34.4 shows plate thermometers

Fig. 34.3 The plate thermometer according to ISO 834 and EN 1363-1 is made of a shielded thermocouple welded to the center of a 0.7-mm-thick Inconel plate, which is insulated on its back side. The exposed front face is 100 mm by 100 mm

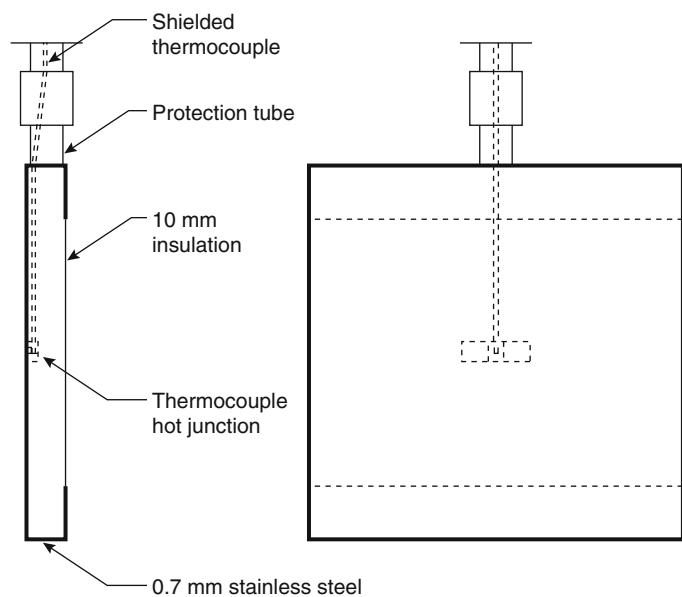




Fig. 34.4 Plate thermometers being mounted around a steel girder for measuring local thermal exposures. Note that the plate thermometers are mounted so that the front

sides of the steel plates are exposed to roughly the same incident radiation as the girder and the back sides are insulated

being mounted at a steel girder with the insulated back side facing the specimen. The front side of the plate thermometer is exposed to approximately the same heating, including radiation conditions, as the specimen. The exposed surface of the plate thermometer is relatively large and, therefore, its sensitivity to convective heat transfer is about the same as that of the specimen surface. The steel plate is thin, only 0.7 mm, and thus responds quickly to temperature changes. As a matter of fact the plate thermometer in a standard fire resistance test measures approximately the temperature of an adiabatic surface (i.e., the temperature of an ideally perfect insulator exposed to the same heating conditions as the specimen surface, as discussed earlier).

The plate thermometer was introduced mainly to harmonize fire endurance tests (see Wickström and Hermodsson [5]), but the measured temperatures are also well suited as input for calculating heat transfer by radiation and convection to fire-exposed surfaces.

As any surface, the plate thermometer surface exchanges heat by radiation and convection. The sum of these equals the transient heat for raising the temperature of the Inconel plate and the backing insulation. Because the plate is thin and does not lose much heat on its back side, this sum is small and can be neglected except for the very first few minutes of a standard test. Thus, the heat balance of the plate can be written as

$$\varepsilon_{PT}(\dot{q}_{inc}'' - \sigma T_{PT}^4) + h_{PT}(T_g - T_{PT}) = 0 \quad (34.16)$$

or

$$\varepsilon_{PT}\sigma(T_r^4 - T_{PT}^4) + h_{PT}(T_g - T_{PT}) = 0 \quad (34.17)$$

The index PT refers to plate thermometer. This means the plate thermometer yields the adiabatic temperature of the specimen for a given surface emissivity and a given convective heat transfer coefficient.

An approximate alternative expression of the net heat transfer \dot{q}_{tot}'' to a specimen surface can now be obtained in terms of one effective temperature only by deducting Equation 34.17 from Equation 34.10:

$$\dot{q}_{\text{tot}}'' = \varepsilon_s \sigma (T_{\text{PT}}^4 - T_s^4) + h(T_{\text{PT}} - T_s) \quad (34.18)$$

In other words the adiabatic surface temperature is approximated by the plate thermometer temperature. This rewriting of Equation 34.10 facilitates the calculations in many cases. The error $\Delta \dot{q}''$ introduced can be quantified by a simple algebraic analysis as

$$\Delta \dot{q}'' = (\varepsilon_s - \varepsilon_{\text{PT}}) \sigma (T_r^4 - T_{\text{PT}}^4) + (h_s - h_{\text{PT}}) (T_g - T_{\text{PT}}) \quad (34.19)$$

Thus, the error is small when the surface emissivity of the plate thermometer and the specimen are nearly the same and when the convective heat transfer coefficients are nearly the same. Therefore, the surfaces of the plate thermometers are blasted and heat-treated before being used to get an emissivity of about 0.8. It also has a relatively large surface, 100 mm by 100 mm, to obtain a convection heat transfer coefficient similar to a specimen. Because T_{PT} always has a value between T_r and T_g , the error vanishes when these two temperatures are close.

Modeling of Heat Conduction in Materials

Heat Conduction in Solid Materials

Heat or energy is conducted in solid materials due to temperature gradients. In one dimension in the x -direction the rate of heat transfer or heat flux is expressed according to Fourier's law as

$$\dot{q}_x'' = -k \frac{\partial T}{\partial x} \quad (34.20)$$

where k is the thermal conductivity.

In fire problems the most usual objective is to determine the temperature distribution in a

structure resulting from conditions imposed on its boundaries. Because these conditions vary with time, the temperature field will be transient or unsteady. It is then governed by the *heat diffusion equation*, which in one dimension is expressed as

$$\frac{\partial}{\partial x} \left(k \frac{\partial T}{\partial x} \right) = \rho c \frac{\partial T}{\partial t} \quad (34.21)$$

where ρ is density, c is specific heat of the material.

If the conductivity k is constant, Equation 34.21 may be written as

$$\frac{\partial T^2}{\partial^2 x} = \frac{1}{\alpha} \frac{\partial T}{\partial t} \quad (34.22)$$

where α is the thermal diffusivity defined as $\alpha = k/\rho c$.

At the boundaries Fourier's law applies and may be expressed as

$$\dot{q}_x''(0) = -k \left. \frac{\partial T}{\partial x} \right|_{x=0} \quad (34.23)$$

Three types of boundary conditions may occur.

1. Given surface temperature: $T(0,t) = T_s$
2. Given surface heat flux: $-k \left. \frac{\partial T}{\partial x} \right|_{x=0} = \dot{q}_s''$
3. Given convection and radiation conditions, for example: $-k \left. \frac{\partial T}{\partial x} \right|_{x=0} = h(T_f - T_s) + \varepsilon \sigma (T_f^4 - T_s^4)$

All the specified boundary conditions, T_s , q_s , and T_f , may vary with time. A special type of heat flux boundary condition is the adiabatic or perfectly insulated surface where q_s is equal to zero.

The heat diffusion equation can be solved analytically only in some uncomplicated cases (see Chap. 2, "Conduction of Heat in Solids," of this book). Numerical methods are usually needed as boundary conditions in general are nonlinear and material properties vary with temperature. There are mainly two types of numerical methods, finite difference and finite element methods, depending on how the geometry is approximated and how the temperature field is

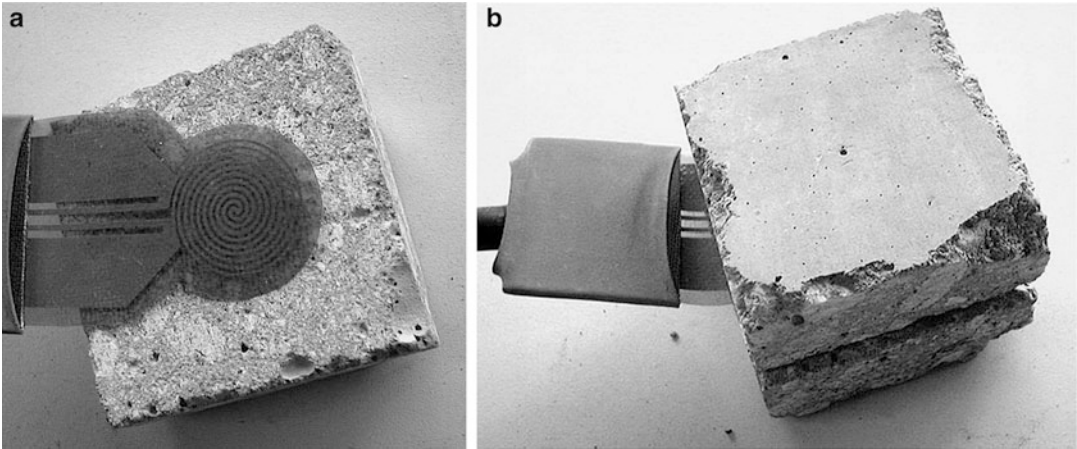


Fig. 34.5 The TPS sensor placed between two pieces of a concrete specimen

expressed by a limited number of discrete temperatures. The finite element method is described briefly later for the one-dimensional case.

Measurement of Thermal Properties

There are a number of techniques to measure thermal properties, each of them suitable for a limited range of materials, depending on thermal properties and temperature level (e.g., see Flynn [6]). However, only a few of the measuring techniques can be used at high temperature levels relevant for fire conditions. They can be divided into steady-state and transient techniques.

The steady-state techniques perform the measurements when the material is in complete equilibrium. Disadvantages of these techniques are that it generally takes a long time to reach the required equilibrium and that at low temperature the measurements are influenced by moisture migration. For moist materials like concrete, it is therefore often preferable to determine the apparent conductivity or thermal diffusivity with transient techniques. These techniques perform the measurements during a process of small temperature changes and can be made relatively quickly.

The guarded hot plate is the most common steady-state method for building materials with a relatively low thermal conductivity [7]. It is

quite reliable at moderate temperatures up to about 400 °C.

Because transient thermal processes dominate in fire safety engineering, the thermal diffusivity, a measure of the speed at which temperature is propagating into a material, is the most interesting parameter. It is naturally best measured with transient methods. One of the most interesting techniques is the transient plane source method (TPS). In this method a membrane, TPS sensor, is located between two specimen halves and acts as a heater as well as a temperature detector (Fig. 34.5). By using this technique, thermal diffusivity, thermal conductivity, and volumetric specific heat can be obtained simultaneously for a variety of materials like metals, concrete, mineral wool, and even liquids and films [8].

Finite Element Calculations of Temperature in Fire-Exposed Structures

When calculating temperature in fire-exposed structures nonlinearities must in most cases be considered. The boundary conditions are nonlinear varying dramatically with temperature as shown above, and also the thermal properties of most materials vary significantly within the wide temperature span that must be considered in fire safety engineering problems. Therefore, numerical methods must be employed. The most general

and powerful codes today are based on the so-called finite element method (FEM).

Basic Equations Derived for One-Dimensional Case

The basic equations that follow are derived for a simple one-dimensional case as an illustration. The same type of equation may be derived for two and three dimensions.

Figure 34.6 shows a wall that has been divided into a number of one-dimensional elements. The temperature between the nodes is assumed to vary linearly along the length.

In any element, interior or at the surface, with length L , conductivity k , and a section area A (Fig. 34.7), the heat flow at the nodes can then be calculated as

$$q_1 = -kA/L*(T_1 - T_2)$$

and

$$q_2 = -kA/L*(-T_1 + T_2)$$

or in matrix format as

$$\bar{q}^e = \bar{k}^e \bar{T}^e \tag{34.24}$$

where \bar{q}^e is the element node heat flow vector, \bar{k}^e is the element heat conduction matrix, and \bar{T}^e is the element node temperature vector. The element heat conduction matrix may then be identified as

$$\bar{k}^e = \begin{Bmatrix} k_{1,1}^e & k_{1,2}^e \\ k_{2,1}^e & k_{2,2}^e \end{Bmatrix} = (kA/L) \begin{Bmatrix} 1 & -1 \\ -1 & 1 \end{Bmatrix} \tag{34.25}$$

and the element nodal temperature and heat flow vectors

as $\bar{T}^e = \left\{ \begin{matrix} T_1 \\ T_2 \end{matrix} \right\}$ and $\bar{Q}^e = \left\{ \begin{matrix} Q_1 \\ Q_2 \end{matrix} \right\}$ respectively.

In a similar way an element heat capacity matrix can be defined by lumping the heat capacity of the element in the nodes. Thus, an element heat capacity matrix may be obtained as

$$\bar{c}^e = \frac{ALcp}{2} \begin{Bmatrix} 1 & 0 \\ 0 & 1 \end{Bmatrix} \tag{34.26}$$

When several elements are combined, the global thermal conductivity matrix \bar{K} can be assembled. In the very simple case of three one-dimensional elements the global heat conduction matrix becomes

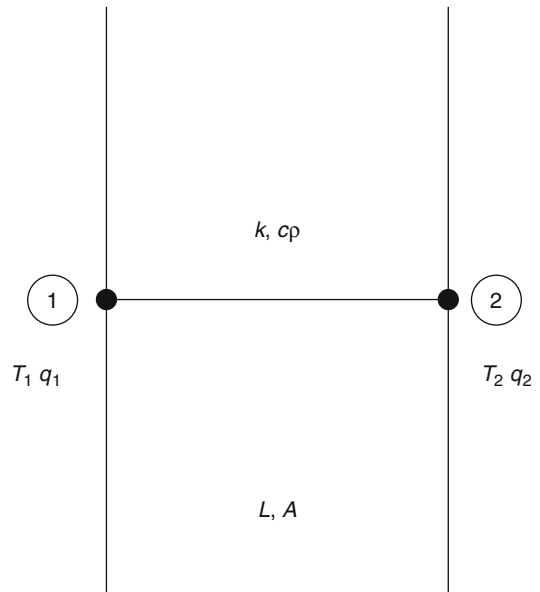
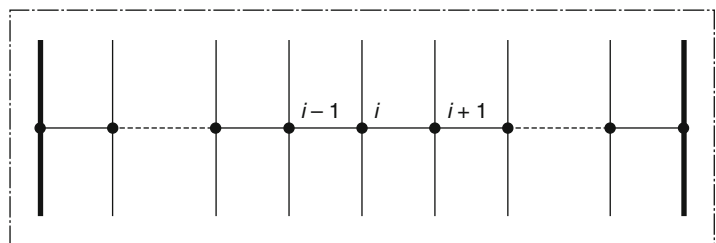


Fig. 34.7 A one-dimensional element with local element node numbers 1 and 2, length L , and a section area A . The element is given a thermal conductivity k , a specific heat capacity c , and a density ρ

Fig. 34.6 A wall divided into one-dimensional elements



$$\bar{K} = \begin{Bmatrix} k_{1,1}^1 & k_{1,2}^1 & 0 & 0 \\ k_{2,1}^1 & (k_{2,2}^1 + k_{1,1}^2) & k_{1,2}^2 & 0 \\ 0 & k_{2,1}^2 & (k_{2,2}^2 + k_{1,1}^3) & k_{1,2}^3 \\ 0 & 0 & k_{2,1}^3 & k_{2,2}^3 \end{Bmatrix} \quad (34.27)$$

where the superscripts 1–3 denote element numbers. The global heat capacity matrix \bar{C} may be assembled in a similar way as the global conductivity matrix. Notice that both the thermal conductivity and the heat capacity matrices are symmetric and dominated by their diagonal elements, and that the global heat capacity matrix assembled from element matrices according to Equation 34.26 will have nonzero elements only in the diagonal. This will have a decisive influence on how the global algebraic heat balance equation can be solved as shown below.

In global form the heat balance equation may now be written as

$$\bar{C}\dot{\bar{T}} + \bar{K}\bar{T} = \bar{Q} \quad (34.28)$$

where $\dot{\bar{T}}$ is the time derivative of the node temperatures. Each row in this equation system represents the heat balance of a node. For each equation or each node either the temperature or the heat flow given in the corresponding rows in the vectors \bar{T} and \bar{Q} , respectively, is known. In principle three options are possible for each equation/row:

1. The node temperature T_i is prescribed.
2. The node heat flow Q_i is prescribed.
3. The node heat flow Q_i can be calculated as a function of a given gas temperature and the surface temperature.

In the first case the corresponding equation vanishes as the unknown quantity is prescribed. The most common case for internal nodes is the second case (i.e., the external flow is zero).

A typical boundary condition when calculating temperature in fire-exposed structures is according to the third option. Based on, for example, Equation 34.11, the external heat flow to the i th node becomes

$$Q_i = A_i \left\{ \epsilon \sigma (T_f^4 - T_i^4) + h(T_f - T_i) \right\} \quad (34.29)$$

where A_i is the section area of the i th node. The differential equation given in Equation 34.28 can be solved numerically by approximating the time derivative as

$$\dot{\bar{T}} = \frac{(\bar{T}^{j+1} - \bar{T}^j)}{\Delta t} \quad (34.30)$$

where \bar{T}^j is the node temperature vector at time step j and Δt is a chosen time increment. Now the heat balance equation in matrix format (Equation 34.28) can be written as

$$\bar{C}(\bar{T}^{j+1} - \bar{T}^j)/\Delta t + \bar{K}\bar{T} = \bar{Q} \quad (34.31)$$

In this differential equation the temperature vector is known at time increment j . The new temperature vector at time $j + 1$ is obtained either explicitly based on the conditions at time step j as

$$\bar{T}^{j+1} = \bar{C}^{-1}(\bar{Q}^j - \bar{K}\bar{T}^j)\Delta t + \bar{T}^j \quad (34.32)$$

or implicitly as

$$\bar{T}^{j+1} = (\bar{C}/\Delta t + \bar{K})^{-1}(\bar{Q}^j + \bar{C}\bar{T}^j/\Delta t) \quad (34.33)$$

Combinations of the solution schemes according to Equations 34.32 and 34.33 are also possible. All such schemes require the solution of an equation system containing as many unknowns as there are unknown node temperatures. Most finite element computer codes use such types of implicit solution schemes. They are numerically more stable than the explicit techniques (i.e., longer time increments may be used).

The explicit solution according to Equation 34.32 may be very simple when the heat capacity matrix \bar{C} is diagonal (i.e., it contains only nonzero elements in the diagonal as shown for a one-dimensional element in Equation 34.26). The solution of the equation system

then becomes trivial because each nodal temperature can be obtained directly/explicitly one at a time. This solution scheme is numerically stable only when the time increment Δt is less than a critical value proportional to the heat capacity over the thermal conductivity of the material times the square of an element length dimension Δx (see Equation 34.34). This requirement applies to all the equations of the entire system. If violated in any of the equations (i.e., at any point of the finite element model), the incremental solution equation will turn unstable.

$$\Delta t_{cr} \approx \frac{cP}{k} (\Delta x)^2 \quad (34.34)$$

A similar condition applies to boundaries of type 3 (e.g., according to Equation 34.29).

This means that short time increments are needed for materials with a low density and a high conductivity and when small elements are used. For information on critical time increments, see Sterner and Wickström [9].

In practice, when calculating temperature in fire-exposed structures, numerical stability is only a problem when modeling sections of thin metal sheets with high thermal conductivity. Then according to Equation 34.34, very short time increments are required. The problem may, however, be avoided by prescribing that nodes close to each other shall have the same temperature. This technique has been applied in the code TASEF [9]. In this code a technique is also developed in which the critical time increment is estimated and thereby acceptable time increments can be calculated automatically at each time step.

Available Computer Codes for Temperature Calculations

Several computer codes are commercially available for calculating temperature in fire-exposed structures. In general modern codes are based on the finite element method. Some are specifically developed and optimized for calculating temperature in fire-exposed structures whereas others are more general-purpose codes.

TASEF [10, 11] and SAFIR [12] are examples of programs that have been developed for fire safety problems. They both for temperature-dependent material properties and boundary conditions. TASEF employs a forward difference solving technique, which makes it particularly suitable for problems in which latent heat due to, for example, evaporation of water must be considered. It yields in most cases very short computing times, in particular for problems with a large number of nodes. Both TASEF and SAFIR have provisions for modeling heat transfer by convection and radiation in internal voids. TASEF can be obtained from TASEF Ltd., UK and SAFIR from the University of Liège, Belgium.

There are many very advanced general-purpose finite element computer codes commercially available such as ABAQUS [13], ANSYS [14], ADINA [15], HEATING [See www.oecd-nea.org/tools/abstract/detail/psr-0199/] and Comsol [16]. The main advantage of using such codes is that they can be used in combination with structural codes and that they come with advanced graphical user interfaces and postprocessors.

Accuracy of Finite Element Computer Codes

At the least the following three steps must be considered when estimating the accuracy of computer codes for numerical temperature calculations:

1. Validity of calculation model
2. Accuracy of material properties
3. Accuracy and reliability of the numerical algorithms of the computer code

The first point is, of course, important. For example, the effects of spalling or water migration cannot be accurately predicted with a code based on just heat transfer according to the Fourier heat transfer equation.

The second point is also crucial. Errors in material property input will be transmitted into output errors. Methods for measuring material properties at high temperature were briefly discussed earlier.

Finally, the numerical verification of the computer code itself is also important. By definition, *verification* is the process of determining that a model implementation accurately represents the developer's conceptual description of the model and the solution to the model [17]. If correctly used, most codes yield results with acceptable accuracy. A scheme to follow including a number of reference cases of various levels of complexity have recently been presented in an SFPE standard [Standard on calculation methods to predict the thermal performance of structural and fire resistive assemblies, please ask Chris Jelenewicz for advice on the status of the standard] partly based on cases earlier suggested by Wickström and Pålsson [18] and Wickström [19]. It is mainly developed for finite element codes but it may also be used for codes based on finite difference principles. The first reference example is a linear problem that can be solved analytically. When increasing the number of elements the results should converge to one correct value. Codes yielding results that converge smoothly when increasing the number of elements are generally deemed reliable for the type of problems considered. The scheme suggested employs problems that are relevant for fire safety engineering, including effects of conductivity varying with temperature, latent heat, radiant heat transfer boundary conditions, and combinations of materials, concrete, steel, and mineral wool. For the development of the SFPE standard the computer codes ABAQUS and TASEF were used to obtain solutions which were deemed reliable as these codes use different solutions algorithms.

Calculation of Temperature in Steel Structures

Metals in general conduct heat very well. The thermal conductivity of steel is on the order of 30 times higher than the corresponding value for concrete and 100–1000 times higher than that of

insulation products. Therefore, the temperature field in a steel section may in many fire engineering cases be assumed uniform. In particular the temperature across the thickness of a steel sheet will be uniform, whereas the temperature in the plane of the sheet may vary considerably, depending on boundary conditions. The methods presented in Chap. 53, “Analytical Methods for Determining Fire Resistance of Steel Members,” assume uniform steel section temperatures. Then zero- or one-dimensional calculation techniques may often be used. For more general two- and three-dimensional cases, numerical computer codes are needed.

Thermal Properties of Steel

The thermal conductivity of carbon steel as a function of steel temperature according to Eurocode 3 [20], is shown in Fig. 34.8. It can also be obtained from Table 34.1.

The specific heat capacity is in most cases more important than the conductivity. In many cases it is accurate enough and convenient to assume a constant specific heat capacity. However, for more accurate calculations the variations with temperature as shown in Fig. 34.9 [20] or given in Table 34.2 are recommended in Eurocode 3 [20]. This specific heat capacity varying with temperature yields in general lower calculated temperatures than when a constant value of 500 J/(kg K) is assumed.

Insulated Steel Structures

In particular in the case of *insulated steel sections* the steel temperature over a section may be assumed uniform. Then the surface heat transfer resistance $1/h_{\text{tot}}$ is in most cases negligible in comparison with the heat resistance (i.e., the thickness over the conductivity of the insulation d_i/k_i). h_{tot} is the combined heat transfer coefficient due to radiation and convection as given in Equation 34.13. The fire-exposed surface temperature is then approximately the same as the

Fig. 34.8 Thermal conductivity of steel as a function of the temperature

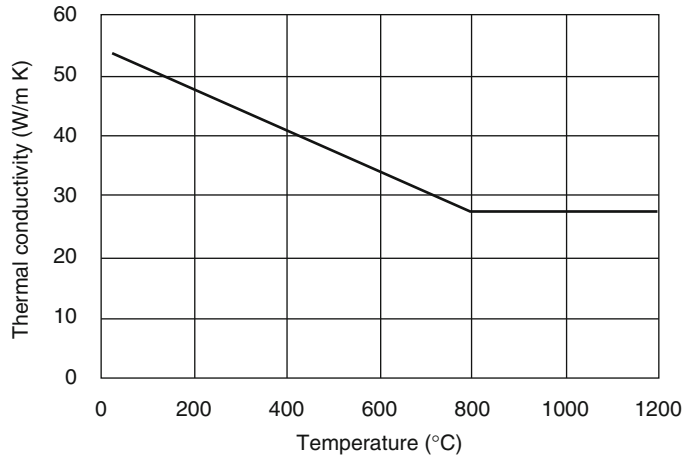


Table 34.1 Thermal conductivity of carbon steel as a function of the temperature [20]

Temperature (°C)	Conductivity (W/m K)
$20 < T_{st} < 800$	$54 - 3.33 \times 10^{-2} T_{st}$
$800 < T_{st} < 1200$	27.3

fire temperature, and the heat transfer to the steel may under steady-state conditions be approximated as

$$q_{tot} = A_s(k_i/d_i)(T_f - T_s) \quad (34.35)$$

where A_s is the fire-exposed area, and T_f and T_s are the fire and steel temperatures, respectively. If the heat capacity of the insulation is negligible in comparison to that of the steel, transient steel temperature can be obtained from the heat balance equation

$$As(k_i/d_i)(T_f - T_s) = c_s\rho_sV_s(\partial T_s/\partial t) \quad (34.36)$$

where c_s and ρ_s are the specific heat capacity and density, respectively, of steel and V_s is the volume per unit length of the considered steel section. In case of heavy insulations when the heat capacity of the insulation cannot be neglected, see the following section on heavily insulated steel structures.

A very simple solution can be obtained if a constant fire temperature rise and constant material properties are assumed; that is,

$$(T_s - T_0) = (T_f - T_0) \left[1 - e^{-(t/\tau)} \right] \quad (34.37)$$

where the characteristic response time or time constant τ of the section is identified as

$$\tau = c_s\rho_sV_s/A_s(k_i/d_i) = (d_i/k_i)(c_s\rho_s)/(A_s/V_s) \quad (34.38)$$

The relation A_s/V_s is denoted the section factor or the shape factor that has the dimension one over length. Instructions on how to obtain this factor for various configurations are given in Table 34.3.

For a fire temperature T_f arbitrarily varying with time or when the material properties vary with temperature, the steel temperature may be obtained (e.g., from the numerical scheme derived from Equation 34.36) as

$$\Delta T_s/\Delta t = (T_f^i - T_s^i)/\tau \quad (34.39)$$

where ΔT_s equals $(T_s^{i+1} - T_s^i)$ and Δt are the steel temperature rise and the time increment, respectively. The superscripts i and $i + 1$ denote the numerical order of the time increments. When the thermal properties vary with temperature, the time constant τ as defined by Equation 34.38 needs to be updated at each time increment. A forward difference solution scheme can be obtained as

Fig. 34.9 Specific heat of steel as a function of the temperature [20]

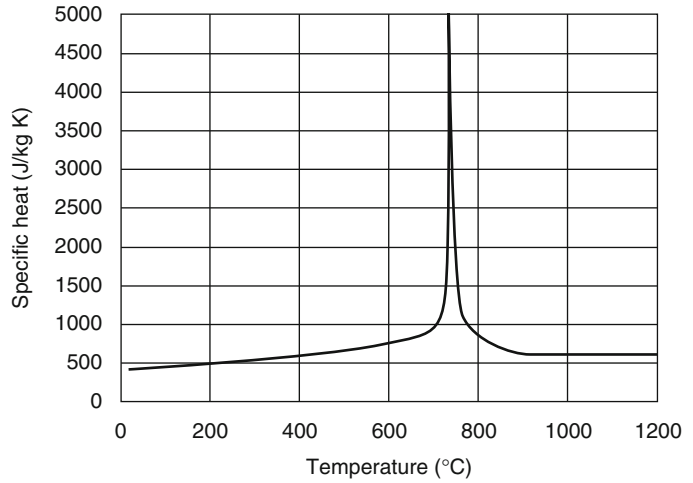


Table 34.2 Specific heat capacity of carbon steel as a function of the temperature [21]

Temperature (°C)	Specific heat capacity (J/[kg K])
$20 < T_{st} < 600$	$425 + 7.73 \times 10^{-1} T_{st} - 1.69 \times 10^{-3} T_{st}^2 + 2.22 \times 10^{-6} T_{st}^3$
$600 < T_{st} < 735$	$666 + 13,002/(738 - T_{st})$
$735 < T_{st} < 900$	$545 + 17,820/(T_{st} - 731)$
$900 < T_{st} < 1200$	650

$$T_s^{i+1} = \Delta t / \tau \cdot T_f^i + (1 - \Delta t / \tau) \cdot T_s^i \quad (34.40)$$

This forward difference scheme is, however, numerically stable only if

$$\Delta t \leq \tau = (d_i / k_i)(c_s \rho_s) / (A_s / V_s) \quad (34.41)$$

This condition must be fulfilled at each time increment. In practice time increments Δt longer than 10 % of that critical value should not be used to ensure accurate results.

Heavily Insulated Steel Structures

The heat capacity of the insulation normally has an insignificant influence on the steel temperature rise rate. However, it will considerably reduce the steel temperature rise of sections protected with relatively heavy insulation. A simple approximative approach is then to lump a third of the heat capacity of the insulation to the steel [22–24]. Equation 34.39 may then be modified as


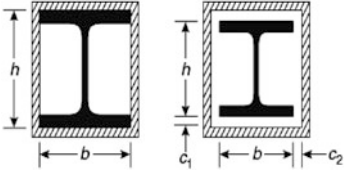
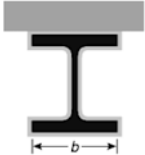
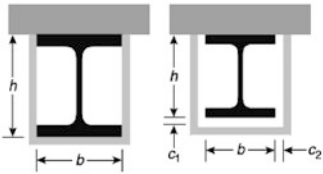
$$\Delta T_s / \Delta t = \left(T_f^i - T_s^i \right) / [\tau(1 + \mu/3)] + [exp(\mu/10) - 1] \Delta T_f / \Delta t \quad (34.42)$$

where μ is the relation between the heat capacity of the insulation and the steel,

$$\mu = (A_i d_i \rho_i c_i) / (V_s \rho_s c_s) \quad (34.43)$$

and where ρ_i and c_i are the density and the specific heat capacity of the insulation, respectively. When the material properties vary with temperature, they may be updated at each time increment. The latter term of Equation 34.42 represents a time delay due to the heat capacity of the insulation. ΔT_f is the fire temperature rise between two time increments. Notice that when the heat capacity of the insulation is much smaller than that of the steel, μ vanishes and Equation 34.42 becomes identical to Equation 34.39.

Table 34.3 Section factor A_s/V_s for steel members insulated by fire protection material [20]

Sketch	Description	Section factor (A_s/V_s)
	Contour encasement of uniform thickness	$\frac{\text{Steel perimeter}}{\text{Steel cross-sectional area}}$
	Hollow encasement of uniform thickness ^a	$\frac{2(b + h)}{\text{Steel cross-sectional area}}$
	Contour encasement of uniform thickness, exposed to fire on three sides	$\frac{\text{Steel perimeter} - b}{\text{Steel cross-sectional area}}$
	Hollow encasement of uniform thickness, exposed to fire on three sides ^a	$\frac{2h + b}{\text{Steel cross-sectional area}}$

^aThe clearance dimensions c_1 and c_2 should not normally exceed $h/4$

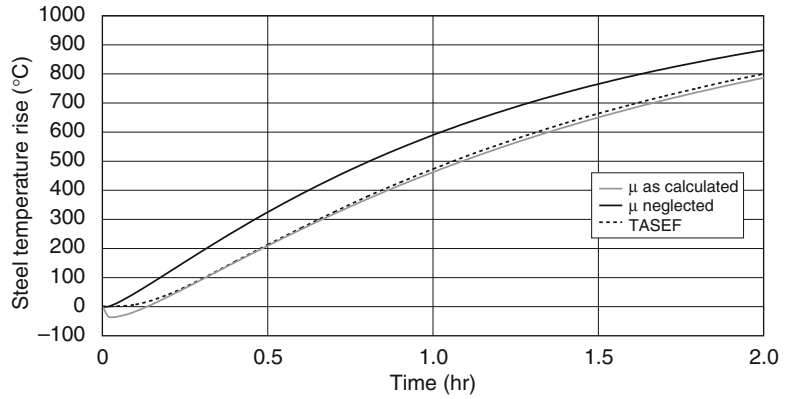
Equation 34.42 has been adopted by Eurocode 3 [20]. The steel temperature can then be obtained, for example, by a forward difference scheme derived from Equation 34.42 as

$$T_s^{i+1} = T_s^i + \Delta t \left(T_f^i - T_s^i \right) / [\tau(1 + \mu/3)] - [exp(\mu/10) - 1] \Delta T_f \tag{34.44}$$

As an illustration of the importance of considering the heat capacity of the insulation, a simple example of a steel section is analyzed considering the relative heat capacity μ of the insulation and for comparison neglecting it (i.e., $\mu = 0$). A section factor $A_i/V_s \approx A_s/V_s = 500 \text{ m}^{-1}$ and an insulation thickness $d_i = 0.05 \text{ m}$, a conductivity

$k_i = 0.2 \text{ W/m K}$, and a specific heat capacity $c_i = 800 \text{ Ws/kg}$ are assumed. Calculated steel temperature developments applying Equation 34.44 considering and not considering the heat capacity of the insulation ($\mu = 0$) are shown in Fig. 34.10. For comparison, temperature rises obtained by accurate finite element calculations are shown as well. Notice how well the temperatures calculated by FEM match the temperatures obtained using the scheme according to Equation 34.44 considering the heat capacity of the insulation. On the other hand, the calculated temperature becomes much higher if the heat capacity of the insulation is not considered. In this case the predicted time to reach a steel temperature of $500 \text{ }^\circ\text{C}$ is on the

Fig. 34.10 Comparison of calculated steel temperature rise of an insulated steel section when exposed to a standard ISO 834 fire exposure, considering and neglecting the heat capacity of the insulation, respectively



order of a quarter of an hour shorter when the heat capacity is not considered. Notice also that Equation 34.44 predicts a negative temperature change for the first 5–10 min, which of course is a numerical error embedded in the equation.

Table 34.4 Constants in the analytical expression of the parametric fire curve

<i>i</i>	0	1	2	3
<i>B_i</i> (°C)	1325	−430	−270	−625
<i>β_i</i> (<i>h</i> ^{−1})	0	−0.2	−1.7	−19

Insulated Steel Structures Exposed to Parametric Fires

Eurocode 3 [20] (EN1991-2-1) has introduced the concept of parametric fires as a convenient way of expressing a set of postflashover design fires. The fire temperature *T_f* is then expressed as (see Eurocode 1 [4])

$$T_f = 20 + 1325(1 - 0.324e^{-0.2t^*} - 0.204e^{-1.7t^*} - 0.472e^{-19t^*}) \tag{34.45}$$

where the modified or scaled time is expressed as

$$t^* = \Gamma t \tag{34.46}$$

and where Γ is a function of the compartment properties (i.e., sizes of openings and thermal properties of enclosure surfaces). A Γ -value approximately equal to unity yields the ISO 834 standard fire, whereas Γ less than unity yields a more slowly growing fire and Γ greater than unity a faster growing fire. The fire duration depends on the fuel density in the fire compartment (see Eurocode 3 [20]). Below it is demonstrated how these types of design fires can facilitate the calculation and the presentation of temperature in fire-exposed insulated steel sections. The concept of parametric fires can also be used for concrete structures using the technique outlined later in this chapter.

When using parametric design fires, the temperature of insulated steel sections can, of course, be obtained by numerical calculations according to Equation 34.40. Then nonlinear phenomena such as temperature-dependent material properties may be considered. However, if the thermal properties are assumed constant and the fire temperature is expressed by exponential terms as in Equation 34.45, then the steel temperature rise as a function of time can be obtained by integration as a closed-form analytic expression [25].

For convenience Equation 34.45 is first written in the form

$$T_s = 20 + \sum_{i=0}^3 B_i \exp(-\beta_i t^*) \tag{34.47}$$

where the constants *B_i* and β_i are given in Table 34.4.

Then the steel temperature can be obtained as a function of the modified fire duration *t** and the modified time constant τ^* of the steel section as

$$T_s - 20 = \sum_{i=0}^3 \frac{B_i}{1 - \beta_i \tau^*} [\exp(-\beta_i t^*) - \exp(-t^*/\tau^*)] \tag{34.48}$$

where

$$\tau^* = \Gamma\tau \quad (34.49)$$

The insulated steel section time constant τ is given in Equation 34.38. The relation between the temperature rise as a function of modified time as expressed in Equation 34.48 is also given in the diagram shown in Fig. 34.11 for various modified time constants τ^* . The diagram in Fig. 34.11 is particularly easy to use for ISO 834 standard fire exposures when Γ by definition is equal to unity.

As an example, consider a steel section with a section factor $A_{st}/V_{st} = 200 \text{ m}^{-1}$ insulated with a 25-mm-thick protection board with a constant thermal conductivity of 0.1 W/(m K). The steel density and specific heat capacity are 7800 kg/m³ and 500 J/(kg K), respectively. The section time constant may then be obtained from Equation 34.38 as $\tau = 4875 \text{ s}$ or 1.35 h. Then if the

section is exposed to standard fire ($\Gamma = 1$), a temperature rise of 418 °C may be obtained from Equation 34.48 or from Fig. 34.11. If the same section is exposed to a more slowly growing fire with $\Gamma = 0.5$, then $\tau^* = \Gamma\tau = 0.68 \text{ h}$ and the temperature rise after 1 h may be found for a modified time of $t^* = \Gamma t = 0.5 \text{ h}$ to be 363 °C. On the other hand, if the section is exposed to a fast-growing fire with $\Gamma = 3.0$, then $\tau^* = (3.0) \cdot (1.35) = 4.05 \text{ h}$ and $t^* = (3.0) \cdot (1.0) = 3.0 \text{ h}$, and the steel temperature rise can be obtained from Equation 34.47 or from Fig. 34.11 as 505 °C. Notice that the maximum steel temperature for a given fire exposure time increases considerably with an increasing Γ -factor. It must, however, also be kept in mind that the fire duration for a given fuel load is proportional to the inverse of the opening factor included in the Γ -factor. For more information see, for example, Eurocode 1 [4].

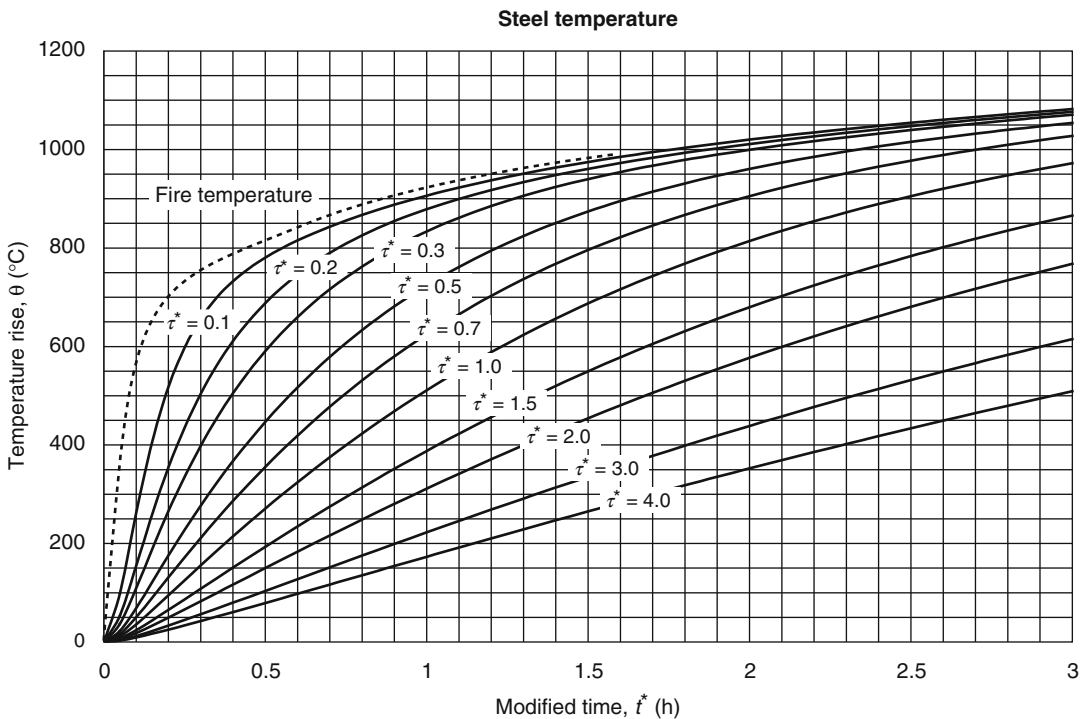


Fig. 34.11 Temperature of various insulated steel sections exposed to parametric fires in the heating phase as a function of modified time t^* . The thermal properties

of the steel sections are expressed in modified time constants τ^* [25]

Unprotected Steel Structures

The temperature of unprotected steel structures is numerically more difficult to calculate as the highly nonlinear heat transfer is decisive for the temperature development of the steel. The total heat transfer q_{tot} may be obtained from Equation 34.11 or Equation 34.12. Then the steel temperature can be obtained from the differential heat balance equation in a similar way as for insulated steel sections (see also Equation 34.36).

$$h_{\text{tot}}(T_f - T_s) = c_s \rho_s (V_s/A_s) (\partial T_s / \partial t) \quad (34.50)$$

where the total heat transfer coefficient h_{tot} may be obtained from Equation 34.13. This equation can be solved numerically with a forward difference scheme in a similar way as for insulated sections as

$$T_s^{i+1} = (\Delta t/\tau) T_f^i + (1 - \Delta t/\tau) T_s^i \quad (34.51)$$

where the characteristic response time τ of the steel section in this case is defined as

$$\tau = c_s \rho_s V_s / A_s h_{\text{tot}} = (c_s \rho_s) / [h_{\text{tot}} (A_s / V_s)] \quad (34.52)$$

Notice that the thermal properties of the steel may vary with temperature, and in particular the total heat transfer coefficient h_{tot} will increase substantially with the temperature level. It would, therefore, be misleading to call τ a time constant in this case.

The stability criterion for the explicit numerical scheme according to Equation 34.51 may then be expressed as

$$\Delta t \leq \tau = (c_s \rho_s) / [h_{\text{tot}} (A_s / V_s)] \quad (34.53)$$

Thus, the critical time increment decreases considerably as h_{tot} increases with time and increasing temperature levels.

Principles for calculating the section factors for various types of configurations of unprotected steel can be found in Table 34.5 [20].

Shadow Effects

When an open section such as an I-section is exposed to fire, the heat transfer by radiation will be partly shadowed (Fig. 34.12). That means the section will only receive as much heat from the fire as if it had the same circumference as a boxed section. Therefore, it is appropriate to replace the area per unit length A_s with the so-called boxed area A_{\square} in Equations 34.50 and 34.52 as the radiation heat transfer mode dominates at elevated temperature. The boxed area A_{\square} is typically for an I-section 30 % less than the corresponding area A_s , which means a proportional increase of the section response time τ . Alternatively, a section with a 40 % higher section factor would yield the same temperature if the concept of shadow effects is applied. This means that by considering the shadow effects in the calculations many more open steel sections can be accepted without thermal protection.

The principal of shadow effects is particularly important for bare, unprotected steel sections, although the concept can be applied to other types of structures as well.

Example of Steel Temperatures Calculated Using Finite Element Codes

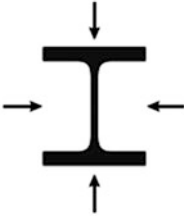
The preceding steel temperature calculations assume uniform steel temperatures in the section analyzed as a crude approximation. It leads indeed in general to solutions on the safe side (i.e., the temperatures are overestimated and often oversized, leading to unnecessary costs). For more precise analyses numerical calculations are needed employing, for example, finite element computer codes. An example is given below.

An encased I-section beam is carrying a concrete slab. It is exposed to standard fire conditions according ISO 834 (Fig. 34.13). Heat transfer conditions according to Equation 34.11 are assumed with $\varepsilon = 0.8$ and $h = 25 \text{ W/m}^2 \text{ K}$. The thermal properties of steel and concrete are

Table 34.5 Section factor A_s/V_s for unprotected steel members [20]

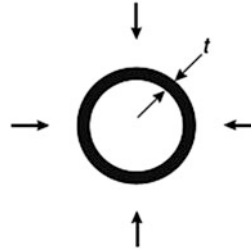
Open section exposed to fire on all sides:

$$\frac{A_s}{V_s} = \frac{\text{Perimeter}}{\text{Cross-sectional area}}$$



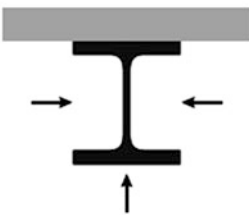
Tube exposed to fire on all sides:

$$A_s/V_s = 1/t$$



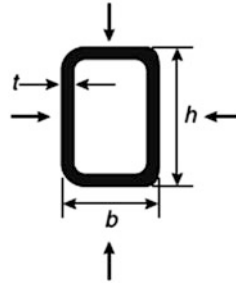
Open section exposed to fire on three sides:

$$\frac{A_s}{V_s} = \frac{\text{Surface exposed to fire}}{\text{Cross-sectional area}}$$



Hollow section (or welded box section of uniform thickness) exposed to fire on all sides:

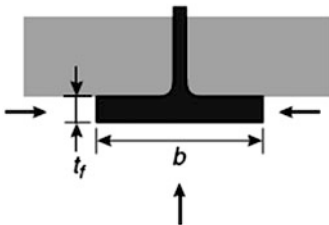
$$\text{If } t \ll b: A_s/V_s \approx 1/t$$



I-section flange exposed to fire on three sides:

$$A_m/V = (b + 2t_f)/(bt_f)$$

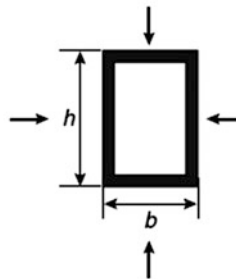
$$\text{If } t \ll b: A_s/V_s \approx 1/t_f$$



Welded box section exposed to fire on all sides:

$$\frac{A_s}{V_s} = \frac{2(b+h)}{\text{Cross-sectional area}}$$

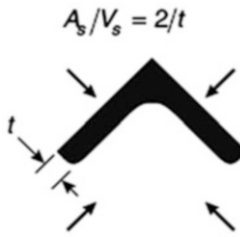
$$\text{If } t \ll b: A_m/V \approx 1/t$$



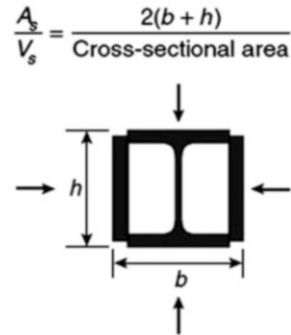
(continued)

Table 34.5 (continued)

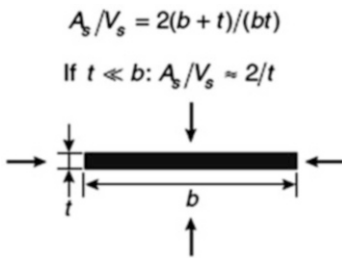
Angle exposed to fire on all sides:



I-section with box reinforcement, exposed to fire on all sides:



Flat bar exposed to fire on all sides:



Flat bar exposed to fire on three sides:

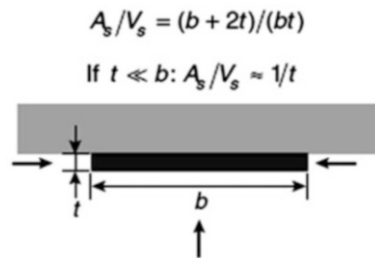
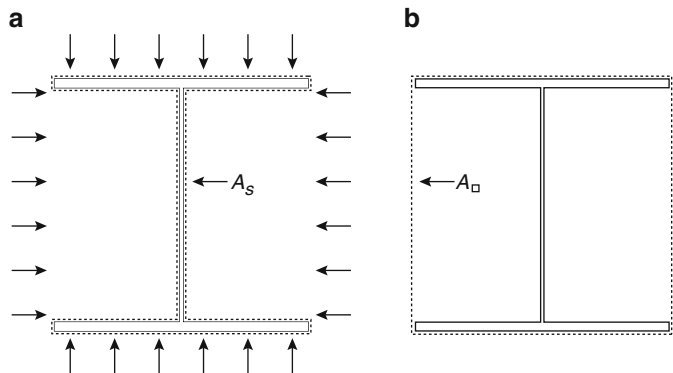


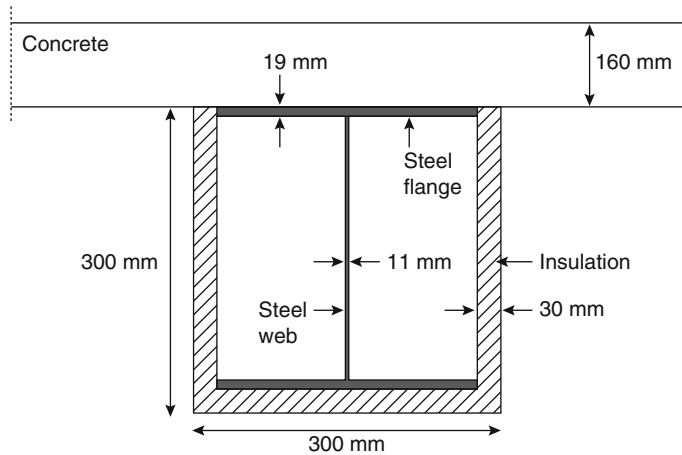
Fig. 34.12 Illustration of the shadow effect. The boxed value area per unit length A_{\square} of a steel section represents the area exposed to heating conditions from the fire



I-section exposed to fire from four sides. The surfaces between the flanges will be partly shadowed.

The boxed area of the I-section, A_{\square} , will have a shorter periphery than the original section.

Fig. 34.13 Encased I-section steel (HE 300B) beam carrying a concrete slab. Slab thickness 160 mm, insulation thickness 30 mm, steel height and width 300 mm, flange thickness 19 mm, and web thickness 11 mm



as given in Eurocodes 2 and 3, respectively, shown above and below. The encasement boards are assumed to have a thermal conductivity (k) of 0.2 W/m K and a volumetric specific heat capacity (c_p) of 40 kJ/m^3 . The finite element discretization model is shown in Fig. 34.14. Heat transfer inside the void is assumed to be by radiation only with an internal surface emissivity of 0.8.

The calculated temperature histories in the steel flanges are shown in Fig. 34.15. For comparison the temperature calculated assuming uniform temperature is also included. Notice that the temperature difference between the minimum and maximum steel temperatures are on the order of $130 \text{ }^\circ\text{C}$ due to uneven heating and steel mass distribution and in particular due to the cooling of the top flange by the concrete slab. A simple approximate calculation can be obtained assuming a uniform steel section temperature, according to the discussion on insulated steel structures, with the section factor calculated as shown in Table 34.3. A time constant τ equal to 6460 s or 1.8 h can then be calculated (Equation 34.38) and a uniform steel temperature after 2 h of about $635 \text{ }^\circ\text{C}$ can be obtained from Fig. 34.10. Notice that this temperature is considerably higher than the average temperature obtained with the much more accurate finite element model.

Calculation of Temperature in Concrete Structures

Reinforced concrete structures are sensitive to fire exposure for mainly two reasons. They may spall due to combinations of internal water pressure and high thermal stresses, and they may gradually lose their load-bearing capacity when the reinforcement bars get hot, reaching temperature levels above $400 \text{ }^\circ\text{C}$. Prestressed steel may even lose strength below that level. In addition the concrete loses both strength and stiffness at elevated temperature. When occurring, spalling usually starts within 30 min of severe fire exposure. Because the spalling phenomenon is very complex and cannot be predicted with simple mathematical temperature models, it will not be further discussed here. Thus, the procedures presented below presume that no spalling occurs that could considerably influence the temperature development.

In general, temperatures in fire-exposed structures may be obtained from tabulated values (see, e.g., Eurocode 2 [26]) or by more or less advanced calculations. Below some simple calculation methods are given. For more general situations, finite element calculations are needed.

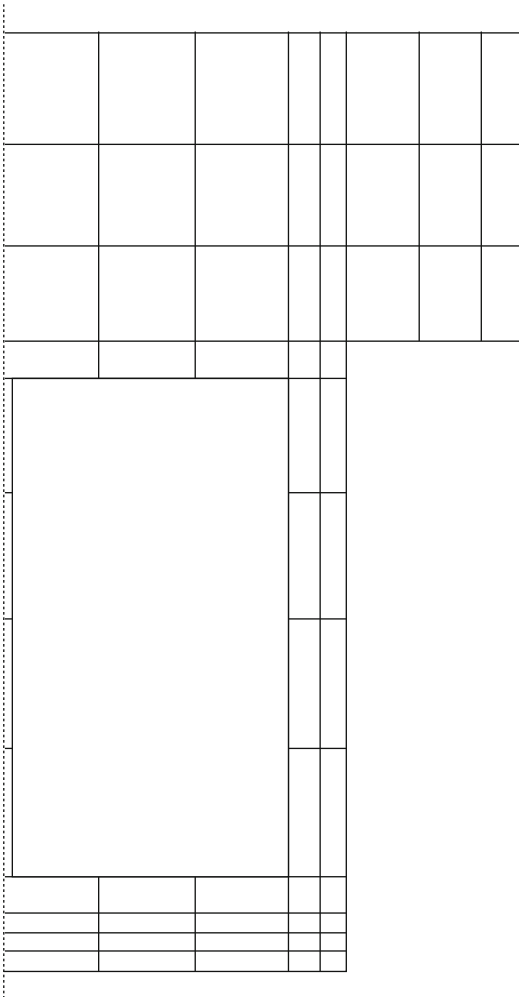
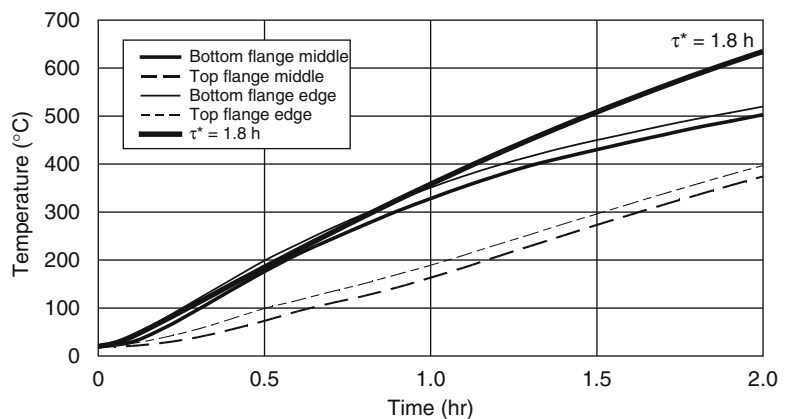


Fig. 34.14 Finite element discretization used to calculate the temperature development of the steel beam shown in Fig. 34.13 when exposed to a standard fire exposure according to ISO 834

Fig. 34.15 Temperature history of bottom and top flanges, middle and corner points



Thermal Properties of Concrete

The thermal conductivity of concrete decreases in general with rising temperature. It depends on concrete quality and type of ballast. For design purposes curves as shown in Fig. 34.16 may be used according to Eurocode 2 [26]. For more accurate calculations with alternative concrete qualities more precise material data may be needed, as discussed earlier.

The specific heat of dry concrete does not vary much with temperature. However, in reality concrete structures always contain more or less physically bound water. This water will evaporate at temperatures above 100 °C and constitute a heat sink as the evaporation consumes a lot of heat. Thus, the specific heat capacity for normal weight concrete according to Eurocode 2 is as shown in Fig. 34.17.

The emissivity of concrete surfaces may be assumed to be 0.8 and the convective heat transfer coefficient may, when simulating fully developed fires, be assumed equal to 25 W/m² K. See, for example, Eurocode 1 [4]. In general the assumed values of these parameters have little influence on calculated temperatures inside concrete structures.

Penetration Depth in Semi-Infinite Structures

Concrete is a material with relatively high density and low conductivity. Therefore, it takes a

Fig. 34.16 Upper and lower limits of thermal conductivity as a function of temperature of normal weight concrete according to Eurocode 2 [26]

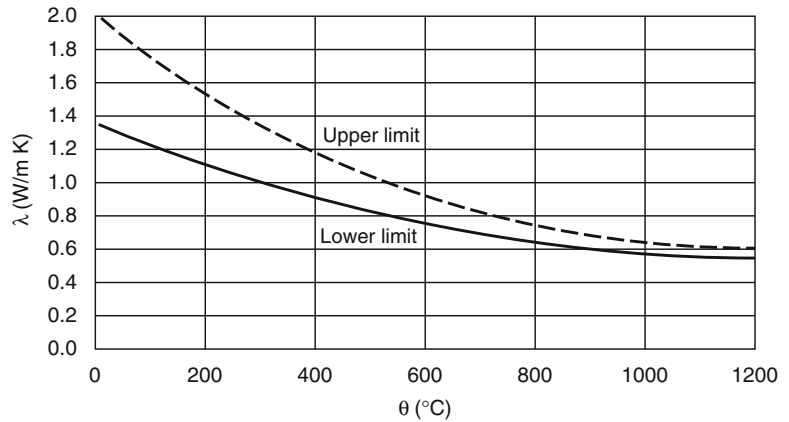
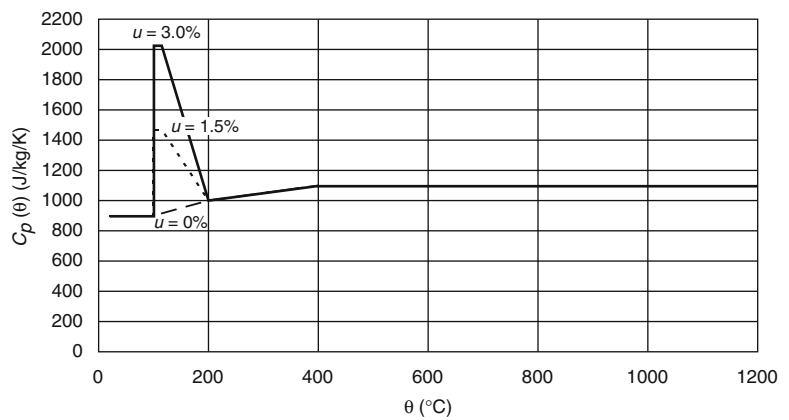


Fig. 34.17 Specific heat capacity of concrete as a function of temperature at three different moisture contents, 0 %, 1.5 %, and 3 %, for siliceous concrete according to Eurocode 2 [26]



long time for heat to penetrate into the structure and raise its temperature, or in other words it takes time before a temperature change at one point is noticeable at another point. Thus, in many cases a concrete structure may then be assumed semi-infinite.

For the idealized case of a semi-infinite body at a uniform initial temperature T_i where the surface temperature momentarily is changed to a constant level of T_s , the temperature rise $(T - T_i)$ inside the body at a depth x at a time t may be written as a function of the normalized group $\eta = x / [2\sqrt{(\alpha t)}]$ where α is an assumed constant thermal diffusivity as defined in Equation 34.22. The relative temperature rise may then be written as

$$\frac{(T - T_i)}{(T_s - T_i)} = erfc(\eta) = 1 - erf(\eta) \quad (34.54)$$

The Gauss complementary error function $erfc$ is shown in Fig. 34.18. Tabulated values of the Gauss error function may be found in textbooks such as Holman [1]. For values of η greater than a value of 1.4 the relative rise is less than 5 %. Thus, depending on accuracy, the temperature penetration depth δ at a given time may be estimated as

$$\delta = 2.8\sqrt{\alpha t} \quad (34.55)$$

As an example, the temperature rise can be estimated to penetrate only about 0.11 m into a concrete structure after 1 h, assuming a

Fig. 34.18 Normalized temperature distribution in a semi-infinite body according to the Gauss complementary error function erfc as in Equation 34.54

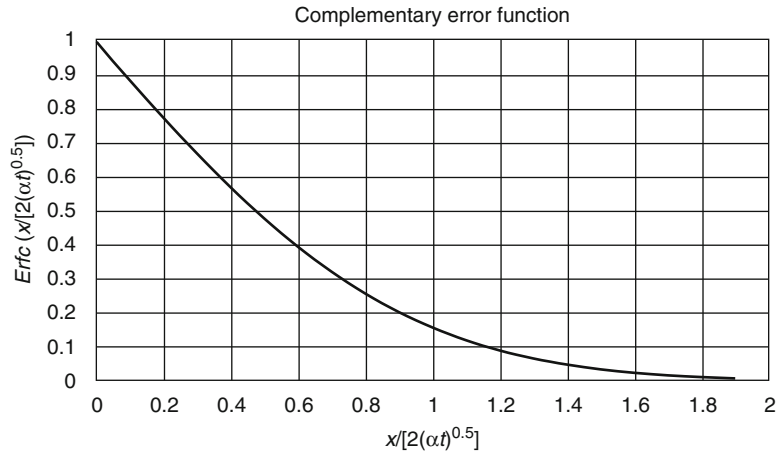
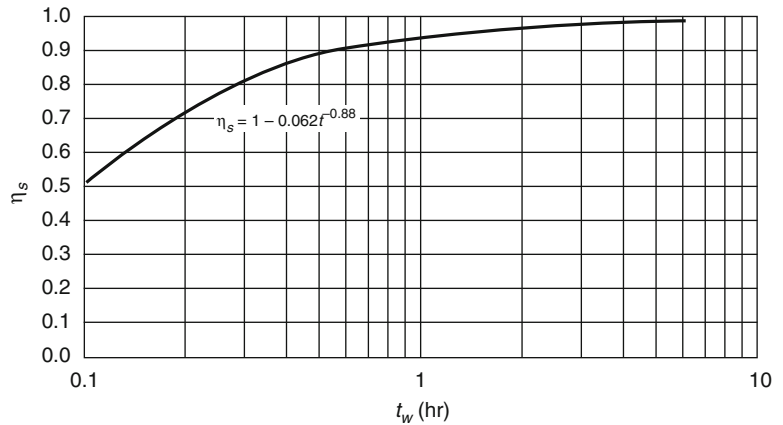


Fig. 34.19 Ratio η_s between concrete surface temperature T_s and the fire temperature T_f as a function of time for a normal weight concrete with thermal properties, according to Eurocode 2 [26], exposed to standard fire conditions, according to ISO 834



conductivity of a 1 W/m K, a density of 2300 kg/m³, and a specific heat capacity of 1000 J/(kg K).

Penetration depth can actually be applied to steel as well. A temperature change at one point of a steel member will not be noticeable beyond a distance corresponding to the penetration depth.

Simple One-Dimensional Calculations

With the thermal properties of concrete as given in the earlier discussion on measurement of thermal properties, the temperature can be calculated in structures exposed to fires. In general, numerical procedures such as finite element methods need to be employed. Wickström [27–29] has, however, shown, based on numerous finite

element calculations, that in one-dimensional cases the temperature inside concrete structures exposed to standard fire conditions according to ISO 834 may be obtained from the diagrams shown in Figs. 34.19 and 34.20. These diagrams apply to normal weight concrete with thermal properties, according to Eurocode 2 [26], as shown in the earlier section on measurement of thermal properties.

In Wickström [27–29] it is shown that the same type of diagrams can be used more generally considering both various parametric fires and various material properties. In these references techniques are also presented on how temperatures can be obtained in walls exposed from two sides and in simple two-dimensional cases by superpositioning based on the same

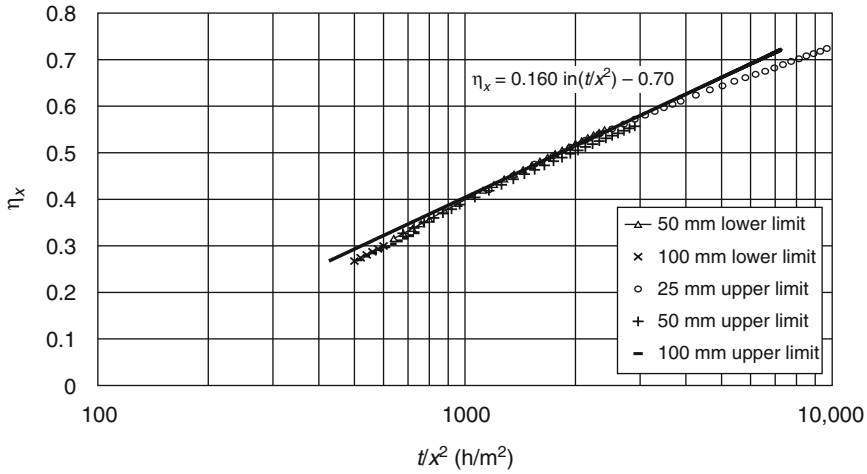


Fig. 34.20 Ratio η_x between internal concrete temperature T_x and the surface temperature T_s as a function of time divided by depth squared t/x^2 for normal weight concrete with thermal properties, according to Eurocode

2 [26], exposed to standard fire conditions, according to ISO 834. Calculations are made assuming the upper and lower limits of the conductivity as shown in Fig. 34.16

simple one-dimensional approximations as outlined below.

Thus, the diagram given in Fig. 34.19 shows the ratio η_s between the concrete surface temperature and the standard fire temperature, according to ISO 834, (see Equation 34.63) as a function of time.

$$\eta_s = \frac{T_s}{T_f} \tag{34.56}$$

The coefficient η_s is in general a function of the group time t over thermal inertia $\sqrt{(k\rho c)}$ of the concrete. In Fig. 34.19 normal weight concrete with thermal properties according to Eurocode 2 [26] is assumed.

Figure 34.20 shows in turn the ratio between the internal temperature T_x at a depth x and the surface temperature T_s . Thus,

$$\eta_x = \frac{T_x}{T_w} \tag{34.57}$$

The coefficient η_x is in principle a function of the Fourier number (i.e., the thermal diffusivity $k/(c\rho)$ of the concrete times the fire duration t over the depth x squared). Results from computer calculations are shown in Fig. 34.20. In these calculations thermal properties of concrete with a water content of 1.5 % are assumed according

to Eurocode 2. Both upper and lower limit values of the conductivity (see Fig. 34.16) are included in the finite element calculations as well as depths of 25, 50, and 100 mm. A straight line is drawn in the logarithmic-linear diagram, which yields approximate temperatures slightly higher than would be obtained with more accurate finite element calculations.

The internal concrete temperature may now be written as

$$T_x = \eta_s \eta_x T_f \tag{34.58}$$

The graphs in Figs. 34.19 and 34.20 can be approximated by simple expressions. Thus,

$$\eta_s = (1 - 0.062t^{-0.88}) \tag{34.59}$$

and

$$\eta_x = [0.16 \ln(t/x^2) - 0.70] \tag{34.60}$$

respectively, where t is time in hours and x is distance in meters from the surface.

Then, in summary, for standard fire exposure according to ISO 834 and normal weight concrete according to Eurocode 2 [26] (see earlier section on thermal properties), a very simple closed-form solution may be obtained for the

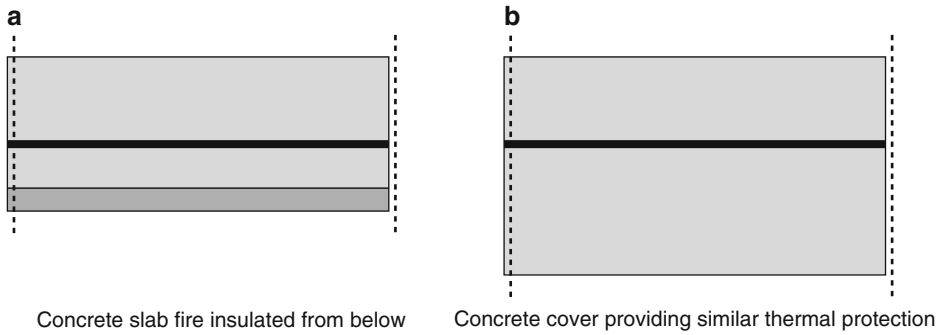


Fig. 34.21 Protection of a concrete structure layer with thickness d_i , which gives an equivalent thermal protection as a concrete layer with thickness d_c

temperature at arbitrary times and depths by inserting Equations 34.59 and 34.63 in hours 34.60 into Equation 34.58:

$$T_x = (1 - 0.062t^{-0.88}) [0.16 \ln(t/x^2) - 0.70] 345 \log(480t + 1) \quad (34.61)$$

As an illustration, the temperature in a slab of normal weight concrete is calculated at a depth of 4 cm when exposed to an ISO 834 standard fire for 1 h. At first η_s is obtained from Fig. 34.19 to be 0.94 for $t = 1$ h. Then for $t/x^2 = 1.0/(0.04)^2 = 625 \text{ h/m}^2$, Fig. 34.20 yields $\eta_x = 0.33$. As the standard time temperature rise after 1 h is $925 \text{ }^\circ\text{C}$, the concrete surface temperature rise is obtained from Equation 34.56 as $0.94 \cdot 925 = 870 \text{ }^\circ\text{C}$ and Equation 34.61 yields the temperature rise at a depth of 4 cm to be $T_x = 0.94 \cdot 0.33 \cdot 925 \text{ }^\circ\text{C} = 287 \text{ }^\circ\text{C}$. A corresponding accurate finite element calculation yields a temperature rise of $T_x = 277 \text{ }^\circ\text{C}$.

Fire-Insulated Concrete Structures

In some applications, it may be advantageous to insulate concrete structure surfaces to prevent them from fast temperature rises. This insulation may either be to avoid spalling or to give the concrete-embedded reinforcement bars additional thermal protection (Fig. 34.21). Behind the protection the temperature of the concrete surface will not rise as quickly as when directly

exposed to fire. Some insulation materials undergo chemical transformations requiring a lot of heat (latent heat) to raise the temperature whereas others work just as passive thermal barriers. Only the latter type of insulation systems is further discussed here and the formula given below only applies to this type of inert material.

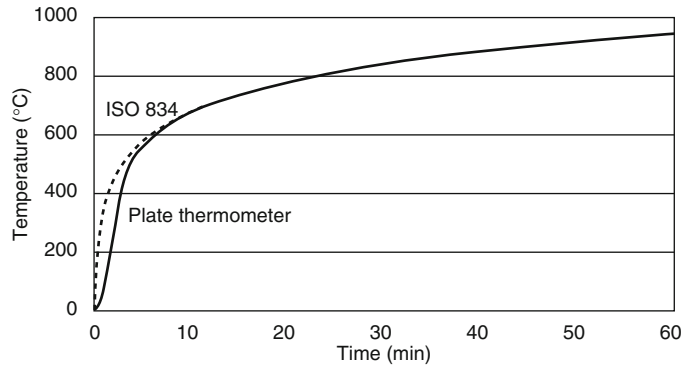
The thermal efficiency of a protection layer is sometimes expressed as the thickness of an additional concrete coverage that would yield the same protection. Wickström and Hadziselimovic [30] have shown that the same effect is approximately obtained when the thermal resistance of the insulation is the same as that for the concrete (i.e., $d_i/k_i = d_c/k_c$ where d is thickness and k conductivity, respectively, and the indices i and c stand for insulation and concrete, respectively). Thus, the equivalent concrete layer thickness can be calculated as

$$d_c = k_c d_i / k_i \quad (34.62)$$

which indicates that the influence of the specific heat capacity and density of the protecting material is negligible in the case of protecting concrete structures. The thermal inertia of the concrete is totally dominating over the inertia of the insulation.

As an example, a 10 mm board of vermiculite with a thermal conductivity of 0.2 W/m K corresponds to a concrete protection layer of 50 mm, assuming the concrete has a conductivity

Fig. 34.22 Calculated response of a plate thermometer when exposed to standard fire test conditions, according to ISO 834, Equation 34.63



of 1.0 W/m K for the temperature interval considered. This could mean considerable savings in both weight and space for a concrete structure.

Calculation of Temperature in Timber Structures

Modeling the thermal behavior of wood is complicated by phenomena such as moisture evaporation and migration, and the formation of char has a decisive influence on the temperature development. Nevertheless, it has been shown that general finite element codes such as SAFIR, TASEF, and COMSOL can be used to predict temperature in fire-exposed cross sections of glued laminated beams [31] provided apparent thermal material properties and appropriate boundary conditions are used. Other specialized numerical codes for timber structures have been developed by Fung [32] and Gammon [33].

More commonly empirical rules are used to estimate the penetration of the charring layer and the loss of strength of timber structures (see, e.g., Eurocode 5 [34]).

Heat Transfer in Fire Resistance Furnaces

Nominal time-temperature relations are clearly defined in fire resistance test standards such as ISO 834, EN 1363-1, and ASTM E119. However, furnaces have various characteristics

depending on the difference between the black body radiation temperature T_r (Equation 34.7) and the gas temperature T_g . In addition there is a time delay of the temperature recording due to the thermal inertia of the monitoring thermocouples. Therefore, when theoretically simulating fire resistance tests, it must be considered how the temperature has been measured in the various standards.

Furnaces Controlled According to ISO 834 and EN 1363-1

In ISO 834 and EN 1363-1 the nominal furnace temperature T_f is given as

$$T_f = 20 + 345 \log_{10}(8t + 1) \quad (34.63)$$

The furnace temperature shall be monitored with plate thermometers (see ISO 834-1 and EN 1363-1). The time delay or, in other words, the time constant of the plate thermometers in a furnace test is negligible, which is indicated in Fig. 34.22, where the calculated temperature response of a plate thermometer exposed to uniform furnace temperature according to ISO 834 is shown. The heat transfer is then calculated according to Equation 34.11 assuming the emissivity ϵ and the convection heat transfer coefficient h equal to 0.9 and 25 W/m² K, respectively.

Notice that the plate thermometer temperature follows the nominal curve very closely except for the first few minutes. Thus, the time delay of the plate thermometer temperature recordings due to inertia in a standard fire test may be neglected

and the heat transfer to a specimen surface can accurately be calculated according to Equation 34.18.

Sometimes it is of interest to know the *incident radiation* level under a furnace test. This level can be measured directly with heat flux meters, but in the section below it is shown how this radiation level may be obtained from plate thermometer measurements.

The incident radiation heat flux q_{inc} may be obtained from Equation 34.16, and plate thermometer temperature recordings given the gas temperature T_g , the emissivity ε_{PT} , and the convection heat transfer coefficient h_{PT} of the plate thermometer are known as

$$q_{inc} = \sigma T_{PT}^4 - h_{PT}(T_g - T_{PT})/\varepsilon_{PT} \quad (34.64)$$

The latter term in Equation 34.64 is relatively small and may be treated as an error term. For values of the emissivity ε_{PT} and the convection heat transfer coefficient h_{PT} equal to 0.8 and 25 W/m² K, respectively, a temperature level of 1000 K and a gas temperature T_g deviating from the plate thermometer temperature T_{PT} by as much as 50 K yields the latter term of Equation 34.64 to be less than 3 %. At higher temperature levels and at minor deviations between gas and radiation temperatures this error is much smaller and probably seldom greater than must be anticipated when measuring incident radiation directly with heat flux meters.

Furnaces Controlled According to ASTM E119

In the American test standard ASTM E119 the nominal furnace temperature is specified according to the time-temperature relation given in Table 34.6.

The standard thermocouple for monitoring the furnace temperature is, however, very thick and, therefore, very slow. According to ASTM E119, it shall have a time constant within the range of from 5.0 to 7.2 min. To eliminate the effects of the time delay the thermocouples may be analyzed as bare steel sections. Thus, by

Table 34.6 Standard Fire Time-Temperature Relation According to ASTM E119

Time (min)	Temperature rise (°C)	Time (min)	Temperature rise (°C)
0	0	90	986
5	556	120	1029
10	659	180	1090
15	718	240	1133
30	821	360	1193
60	925		

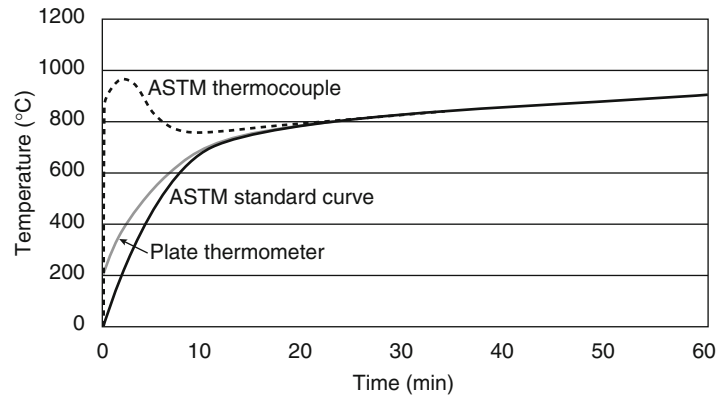
applying Equation 34.51, the effective fire temperature T_f can be derived from the corresponding thermocouple measurements T_{tc} as

$$T_f^{i+1} = T_{tc}^{i+1} + \tau/\Delta t (T_{tc}^{i+1} - T_{tc}^i) \quad (34.65)$$

The furnace thermocouple time constant, as referred to in the ASTM E119 standard, is rather imprecisely specified as the heat transfer by radiation that is nonlinear and increases by the temperature level raised to the fourth power. More realistic is to assume a time constant of 6 min (in the middle of the range from 5.0 to 7.2 min) at a furnace temperature level of perhaps 1000 K, and then obtain the heat transfer to the thermocouple by calculating the heat transfer according to Equation 34.11 assuming ε and h equal 0.9 and 50 W/m² K, respectively. Then match a surface-to-volume ratio obtained from Equations 34.52 and 34.13 to obtain the stipulated time constant. (As a comparison, the corresponding time constant for a plate thermometer at the same temperature level is on the order of 15 s.)

Figure 34.23 shows the actual furnace temperature rise in a furnace controlled ideally precisely according to ASTM E119. Notice that the real or effective furnace temperature is much higher than indicated by the slowly responding ASTM type of shielded thermocouples. It must, however, be noted that the above analysis assumes that the furnace radiation and gas temperatures are equal, which is seldom the case. The gas temperature may be higher than the radiation temperature and, therefore, the differences in practice between the ASTM thermocouple and the plate thermometer may be much less, as the

Fig. 34.23 Temperatures ASTM E119 and ISO 834 (plate thermometer), respectively, must follow to obtain the effective furnace temperature T_f according to ASTM E119 due to time delay



ASTM thermocouple is more sensitive to convective heat transfer than the plate thermometer. The general observation from this theoretical analysis agrees with the test results reported by Sultan [35]. The difference between the ASTM type of thermocouples and the plate thermometer is insignificant after 10 min.

References

1. J.P. Holman, *Heat Transfer*, 4th ed., McGraw Hill, New York (1976).
2. U. Wickström, D. Duthinh, and K.B. McGrattan, "Adiabatic Surface Temperature for Calculating Heat Transfer to Fire Exposed Structures," Interflam, Interscience Communications, London, UK (2007).
3. K.B. McGrattan, S. Hostikka, J.E. Floyd, H.R. Baum, and R.G. Rehm, *Fire Dynamics Simulator (Version 5), Technical Reference Guide*, NIST SP 1018-5, National Institute of Standards and Technology, Gaithersburg, MD (2005).
4. EN 1991-1-2, "Eurocode 1: Actions on structures—Part 1-2: General Actions—Actions on Structures Exposed to Fire," European Committee for Standardization (CEN), Brussels, Belgium (2002).
5. U. Wickström and T. Hermodsson, T., "Comments on Paper by Kay, Kirby, and Preston, 'Calculation of the Heating Rate of an Unprotected Steel Member in a Standard Fire Resistance Test,'" *Fire Safety Journal*, 29, 4, pp. 337-343 (1997).
6. D. Flynn, "Response of High Performance Concrete to Fire Conditions: Review of Thermal Property Data and Measurement Techniques," NIST GCR 99-767, National Institute of Standards and Technology, Gaithersburg, MD (Mar. 1999).
7. ISO 8302:1991, Thermal insulation -- Determination of steady-state thermal resistance and related properties -- Guarded hot plate apparatus.
8. B. Adl-zarrabi, L. Boström, and U. Wickström, "Using the TPS Method for Determining the Thermal Properties of Concrete and Wood at Elevated Temperature," *Fire and Material*, 30, pp. 359-369 (2006).
9. E. Sterner and U. Wickström, "TASEF—Temperature Analysis of Structures Exposed to Fire," SP Report 1990:05, Swedish National Testing and Research Institute, Borås, Sweden, (1990).
10. U. Wickström, "TASEF-2—A Computer Program for Temperature Analysis of Structures Exposed to Fire," Ph.D. Dissertations, Lund Institute of Technology, Department of Structural Mechanics, Report No. 79-2, Lund, Sweden (1979).
11. E. Sterner and U. Wickström, "TASEF—Temperature Analysis of Structures Exposed to Fire," SP Report 1990:05, SP Technical Research Institute of Sweden, Borås, Sweden (1990).
12. J.M. Fransén, V.K.R. Kodur, and J. Mason, "A Computer Program for Analysis of Structures Submitted to Fire," *User's Manual of SAFIR 2001*, University of Liege, Belgium (2000).
13. *ABAQUS Standard User's Manual, volumes I-III, version 6.2*, Hibbit, Karlsson and Sörensen, Inc., Pawtucket, RI (2001).
14. ANSYS, Inc., 275 Technology Drive, Canonsburg, Pennsylvania (<http://www.ansys.com>).
15. K.J. Bathe, *Finite Element Procedures*, Prentice Hall, Upper Saddle River, NJ (1996).
16. See website <http://www.comsol.com>.
17. *Guide for Verification and Validation of Computational Fluid Dynamics Simulations*, AIAA, Guide G-077-1998, American Institute of Aeronautics and Astronautics, Reston, VA (1998).
18. U. Wickström and J. Pålsson, "A Scheme for Verification of Computer Codes for Calculating Temperature in Fire Exposed Structures," SP Report 1999:36, Swedish National Testing and Research Institute, Borås, Sweden (1999).
19. U. Wickström, "An Evaluation Scheme of Computer Codes for Calculating Temperature in Fire Exposed Structures," Interflam (1999).
20. EN 1993-1-2, "Eurocode 3: Design of Steel Structures—Part 1-2: General Rules—Structural

- Fire Design,” European Committee for Standardization (CEN), Brussels, Belgium (2005).
21. J. Hamann, R. Müller, R. Rudolphi, R. Schriever, and U. Wickström, “Anwendung von Temperatur-Berechnungsprogrammen auf kritische Referenzbeispiele des Brandschutzes,” Bundesanstalt für Materialforschung und -prüfung, Berlin (1999).
 22. U. Wickström, “Temperature Analysis of Heavily-Insulated Steel Structures Exposed to Fire,” *Fire Safety Journal*, 5, pp. 281–285 (1985).
 23. S.J. Melinek and P.H. Thomas, “Heat Flow to Insulated Steel,” *Fire Safety Journal*, 12, pp. 1–8 (1987).
 24. Z.H. Wang and H.T. Kang, “Sensitivity Study of Time Delay Coefficient of Heat Transfer Formulations for Insulated Steel Members Exposed to Fires,” *Fire Safety Journal*, 41, pp. 31–38 (2006).
 25. U. Wickström, “Temperature Calculation of Insulated Steel Columns Exposed to Natural Fire,” *Fire Safety Journal*, 4, pp. 219–225 (1981).
 26. EN 1992-1-2, “Eurocode 2: Design of Concrete Structures—Part 1–2: General Rules—Structural Fire Design,” European Committee for Standardization (CEN), Brussels, Belgium (2004).
 27. U. Wickström, “A Very Simple Method for Estimating Temperature in Fire Exposed Concrete Structures”, in *Proceedings of New Technology to Reduce Fire Losses & Costs*, (S.J. Grayson and D.A. Smith, eds.), Elsevier, New York (1986).
 28. U. Wickström, “Application of the Standard Fire Curve for Expressing Natural Fires for Design Purposes,” *Fire Safety: Science and Engineering*, ASTM STP 882, American Society of Testing and Materials, Philadelphia, pp. 145–159 (1985).
 29. U. Wickström, “Natural Fires for Design of Steel and Concrete Structures—A Swedish Approach,” *International Symposium on Fire Engineering for Building Structures and Safety, the Institute of Engineers, Australia*, National Conference Publication No. 89/16, Melbourne (1989).
 30. U. Wickström and E. Hadziselimovic, “Equivalent Concrete Layer Thickness of a Fire Protection Insulation Layer Paper,” *Fire Sa, Brandteknik*, Odense, Denmark (1996).
 31. B.L. Badders, J.R. Mehaffey, and L.R. Richardson, “Using Commercial FEA software Packages to Model the Fire Performance of Exposed Glulam Beams,” *Fourth International Workshop “Structures in Fire,” Aveiro, Portugal* (2006).
 32. F.C.W. Fung, “A Computer Program for the Thermal Analysis of the Fire Endurance of Construction Walls,” *NBSIR 77.1260*, National Bureau of Standards, Washington, DC (1977).
 33. B.W. Gammon, “Reliability Analysis of Wood-Frame Wall Assemblies Exposed to Fire,” Ph.D. Dissertation, University of California, Berkeley (1987).
 34. EN 1995-1-2, “Eurocode 5, Design of Timber Structures—Part 1–2: General Rules—Structural Fire Design,” European Committee for Standardization (CEN), Brussels, Belgium (2004).
 35. M.A. Sultan, “A Comparison of Heat Exposure in Fire Resistance Test Furnaces Controlled by Plate Thermometers and by Shielded Thermocouples,” *Interflam 2004*, Edinburgh, Scotland, pp. 219–229 (2004).

Professor Ulf Wickström is teaching heat transfer in fire technology at Luleå University of Technology, Sweden. He is a former head of the Department of Fire research at SP Technical Research Institute of Sweden. Professor Wickström has a PhD from Lund University of Technology in fire technology and a master of science from the University of California, Berkeley. For his thesis research he developed the computer program TASEF for calculating temperature in fire-exposed concrete and steel structures. His focus of scientific interest is heat transfer analysis of structures exposed to fire, on which he has published several papers.